Chap.4: Hybrid organic-inorganic perovskites: a spin-off of oxidic perovskites

Alberto García-Fernández (1), Emilio José Juárez-Pérez (2), Socorro Castro-García (1), Manuel Sánchez-Andújar (1), María Antonia Señarís-Rodríguez (1).

(1) QuiMolMat group, Department of Fundamental Chemistry, Faculty of Science and Centro de Investigaciones Científicas avanzadas (CICA), University of A Coruña, Campus A Coruña, 15071 A Coruña, Spain

(2) ARAID Foundation, Institute of Nanoscience of Aragon (INA), University of Zaragoza. 50018 Zaragoza, Spain

Corresponding author: m.senaris.rodriguez@udc.es

Abstract: ABX_3 compounds with perovskite structure have been intensively and extensively studied in the last decades in view of their structural richness and amazing variety of interesting properties, such as piezoelectricity, ferroelectricity, ferromagnetism, superconductivity, magnetoresistance, multiferroicity, etc. In this chapter, we recompile well-established chemical and structural concepts in pure inorganic perovskites (mainly oxidic perovskites), and extend them to the young family of hybrid organic-inorganic perovskites. Our final goal is to help understanding the relationships among composition, crystal structure and properties in this new family of compounds, for inspiring further the design of novel materials.

Keywords: PEROVSKITE STRUCTURE, HYBRID ORGANIC-INORGANIC PEROVSKITES, PEROVSKITE-RELATED STRUCTURES, DISTORTIONS MECHANISMS, STRUCTURE-PROPERTY RELATIONSHIPS.

Cite this paper: A. García-Fernández, E.J. Juárez-Pérez, S. Castro-García, M. Sánchez-Andújar, M.A. Señarís-Rodríguez, DOI:10.23647/ca.md20202205

A. García-Fernández, E.J. Juárez-Pérez, S. Castro-García, M. Sánchez-Andújar, M.A. Señarís-Rodríguez

I. Introduction

Compounds with general formula ABX_3 and perovskite structure have been intensively studied since the middle of the twentieth century because of their interesting functional (1) and multifunctional properties, such as, ferroelectricity and piezoelectricity,(2) magnetism,(3) superconductivity,(4) multiferroicity,(5) magnetoresistance,(6) catalytic (7) and optical properties (1). Such studies, carried out over several decades mainly on oxidic perovskites ABO_3, have allowed the establishment of important concepts that relate the composition and the crystalline structure of these compounds with their properties. (8)

Among the very-well known characteristics of perovskites, a very remarkable one is their composition diversity and structural flexibility to support multiple substitutions into all the A-, B- and X-sites.(9) Such peculiar and amazing behaviour, by which they received the title of “chemical chameleons”, (10)(11) has more recently allowed to design novel perovskites with a myriad of building blocks, such as molecular components of inorganic and even organic nature. Thus, new and more complex members of the perovskite family have emerged over the past years. In this context, especially relevant are the so-called hybrid organic-inorganic perovskites (HOIPs) or “molecular” perovskites, which are currently a hot spot due to their interesting and even unprecedented functional and multifunctional properties, including photovoltaic and optoelectronic properties, magnetism, dielectricity, ferroelasticity, ferroelectricity and multiferroicity.(12) The most obvious advantage of such organic–inorganic hybrids is that they can favourably combine the often dissimilar properties of organic and inorganic components in one material. Due to the large variety for possible combinations of components this field is very creative, since it provides the opportunity to prepare an almost unlimited set of new materials with large structural and behavioural diversity. Another driving force in the area of hybrid perovskites is the possibility to create (multi)functional (13) and (multi)stimuli responsive materials, in which the application of a single or multiple external stimuli is able to induce specific functionalities. These possibilities clearly reveal the power of hybrid materials to generate complex systems from a simple building blocks approach.

But probably the most intriguing characteristic of hybrid perovskites, which makes them so interesting for many applications, is their easy fabrication and processing. Unlike pure inorganic perovskites, such as the oxidic perovskites, that often require high temperature treatments for their synthesis and processing, hybrid (mostly halide type) perovskites can be obtained by solution and low temperature processing. Hence, these materials can be conformed in any form in bulk (14) and nanostructured (thin-

films or nanoparticles) (15) by a simple solution process, which leads to an easy and cheap conforming by a simple chemical treatment.

Therefore, the combination of interesting (multi)functional properties and low cost processing, reveals a promising future for hybrid perovskites and their use in the next generation of technological devices and many energy and environmental applications.

The aim of this chapter is to provide to the reader an overview of the large knowledge already existing about pure inorganic and hybrid (halide) perovskites, with emphasis in chemical and structural aspects as they are of primary importance for full understanding of their physical properties. For this purpose, we will first begin with the case of oxidic perovskites to subsequently focus on hybrid perovskites taking into account well-established concepts in inorganic perovskites, as well as novel characteristics innate of hybrid perovskites.

II. Inorganic perovskites

Perovskite is a mineral composed of calcium titanate ($CaTiO_3$). Perovskite-group minerals have a great interest to Geophysics (16), for example, $MgSiO_3$ silicate perovskite is one of the most abundant minerals in the lower part of Earth's mantle.(17) Also, a perovskite is any synthetic material with the same type of crystal structure as $CaTiO_3$ mineral, known as the perovskite structure. In addition to naturally-occurring materials, synthetic materials with perovskite structure are one of the most common and most extensively studied in solid state chemistry and physics and materials science. In fact, there is a huge number of synthetic materials that display this crystal structural type under the general chemical formula ABX_3, in which A and B are metal cations of different sizes (being the A-site cations usually larger than the B-site cations) and X are anions that bridge two B cations (see Figure 1). A wide variety of cations/anions may be incorporated, each with different valence, so long as charge neutrality is satisfied.

Historically, the oxide-based perovskites (ABO_3), where the X anion is O^{2-} and more than 25 (50) cations can occupy the A (B) site, have been the most actively studied perovskite family due to their vast and interesting functional properties, such as ferroelectricity,(18) magnetism,(19) (20) superconductivity,(21) magnetoresistance (22) and catalytic properties.(23) We will be mainly referring to them in this section devoted to inorganic perovskites.

In any case, among other known inorganic perovskites are ABX_3 compounds where X is a halide (F^-, Cl^-, Br^- and I^-), sulphide, selenide, oxynitride, hydride and even tetrahydroborate anion.

The idealised or aristotype perovskite structure ABX_3 is cubic with space group $Pm\bar{3}m$ and cubic close packing of "AX_3" layers. There are two general ways for depiction of the unit cell. In the first one, the A cations are shown at the cube corners, the B cations in the body centre and the X anions at the face centres of the cube (Figure 1a). In the second one, the A cations are shown at the body centre, the B cations at the cube corners and the X anions at the edge centres (Figure 1b and c). Both descriptions are interchangeable and are simply related by translation of the origin half way along the cube body diagonal, setting the cell origin either on the A- or B- cations, respectively. As it can be seen in Figure 1b, the larger A cations are surrounded by 12 X ions, in a cubooctahedral coordination, while, the smaller B cations have a regular octahedral coordination of X anions, where the six B-X bond lengths are equal and the six X-B-X bonds are linear.

Alternatively, the structure can also be described as built-up from an array of $[BX_6]$ octahedra, which share all corners in the three directions of the space and give rise to a three dimensional (3D) framework, with the A cations located in the resulting cubooctahedral cavities (Figure 1c).

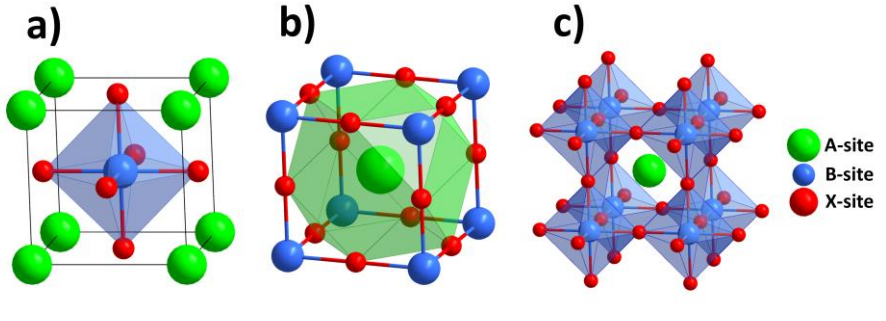

Figure 1: The idealized ABX_3 perovskite structure, displayed with A (a) or B (b,c) at the center of the cube, and visualizing the octahedral B-site coordination (a,c) and the cuboctahedral A-site coordination (b).

This seemingly simple atomic arrangement –which in turn allows a relatively easy correlation between the properties and the crystalline structure- is the basis for a plethora of different materials with an exceptional diversity of physical and chemical properties.

Such a versatility of the perovskite structure relies mainly on three facts: Firstly, this structure can accommodate a large number of possible elements for the A, B and even X position, even with more than one in each of these sites, spanning a large portion of the periodic table. Secondly, the initially ideal cubic structure can be distorted in

several different ways, e.g., by tilting of the octahedra or by displacing the cations from the centre of their polyhedral also enlarging the number of possible polymorphs.(24) Also, the structure is able to accommodate a rather large non-stoichiometry, giving rise to new phases and new properties.

II.1 Goldschmidt tolerance factor

From a crystallographic perspective, the ideal cubic structure of perovskite is inflexible, as the unit cell has no adjustable atomic position parameters, so that any compositional change must be accommodated by a change in the lattice parameter, which is a simple sum of anion-cation bond lengths. In the ideal cubic perovskite ABX_3, the A-X (A-O) bond length equals to the $\sqrt{2}$*B-X (B-O) bond length, based on simple geometric considerations. However, it is rather unusual that the A and B cation radii match perfectly allowing a rather large size mismatch of ionic radii in the structure.

This A ,B and X size match or mismatch is often described by the Goldschmidt tolerance factor, *TF* (25) (Equation 1),which allows to predict the stability of the perovskite structure based on the size of the given ions:

$$TF = \frac{r_A + r_X}{\sqrt{2}(r_B + r_X)} \qquad \text{Eq. 1}$$

where r_A, r_B and r_X are the effective ionic radii of the A, B and X ions, respectively.

In the ideal cubic perovskite structure, *TF* should be strictly equal to 1.0. Nevertheless, it has been found empirically that if *TF* lies in the approximate range 0.9–1.0 a cubic perovskite structure is a reasonable possibility.

In the cases where *TF* is of the order of 0.71–0.9, the perovskite structure will still form, but the structure -specially the octahedral framework- will distort to accommodate for the A, B, O^{2-} mismatch. Such distortions will lower the initially cubic symmetry of the structure and give rise to rhombohedral, orthorhombic, etc., perovskites depending on the value of *TF*.(8)

For even lower values of *TF*, that is when the size of the A cation has decreased becoming more similar to that of B, the perovskite structure is no longer stabilized, and the ilmenite crystalline structure forms instead, with both the A and B cations in octahedral coordination.

On the other hand, if *TF* > 1, that is, if a relatively too large A and a relatively too small B are present, a hexagonal packing of the "AX_3" layers is preferred instead of the cubic one presented so far, and hexagonal phases are formed, with a framework based in face-sharing octahedra (see more information in p. 11).

Before ending this section is worth noting that, very recently, a new way to calculate the tolerance factor (τ) of oxidic and halide perovskites has been presented, which according to their authors is more accurate than the Goldschmidt tolerance factor.(26)

This new tolerance factor (τ) has the form:

$$\tau = \frac{r_X}{r_B} - n_A\left(n_A - \frac{r_A/r_B}{\ln(r_A/r_B)}\right) \qquad \text{Eq. 2}$$

where n_A is the valence of A cation, and r_A and r_B are the ionic radii of A and B cations. According to this new tolerance factor, the perovskite structure is stable when $\tau < 4.18$.

II.2 Distortions of the perovskite structure

As already mentioned, the mismatch in the sizes of A, B and X results in structural distortions of the perovskite structure which, in turn, have a profound influence on the physical properties of these materials.

For instance, if *TF* < 1, the A-site cation radius is smaller (B-site cation radius is larger) than ideal, and the perovskite structure compensates for the cation size mismatch by tilting the [BX_6] octahedra. In this situation, the B-X bonds will undergo compression, and the A-X bonds tension, to compensate for the excess space (void). A rotation of the [BX_6] octahedra accommodates these induced stresses, leading a tilting of the octahedra and a reduction of the symmetry (Figure 2). As the octahedra are sharing the corners, their rotation is cooperative and restraint. The possible octahedral networks derived from those rotations are well known and classified using the Glazer notation. (27)

A direct consequence of these distortions is the deviation of the B-X-B angles from 180º, factor that has a huge impact in the electronic characteristics of the compound (for example on its electronic bandwidth, and therefore on the degree of electronic localization/delocalization) or on the nature of its magnetic interactions. (28)

Additionally, mismatch of ions can induce cation displacements (Figure 2), with the A cation simply shifted away from the centre of the cuboctahedral site, or the B cations shifted from the centre of the octahedral site. In this latter, the [BX_6] can distort to give elongated or flattened octahedra, distortion that is particular enhanced for transition metals that can exhibit a Jahn-Teller effect, also with direct impact in physical properties.

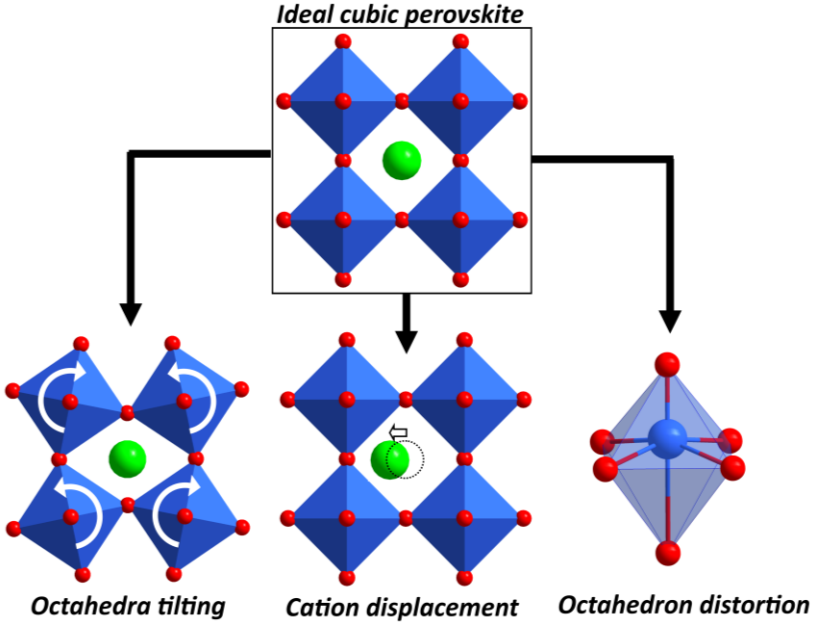

Figure 2: Ideal cubic ABX_3 perovskite structure and its common structural distortions (namely: octahedral tilting, cation displacement and octahedron distortion) induced by the mismatch at the size of the ions.

These three structural distortions, namely, cation displacement, [BX_6] tilt/rotation and [BX_6] distortion, are not mutually exclusive and they can occur independently or, often, in combination with each other.

II.3 Compounds with perovskite and related structures

Along the last decades, the extensive studies on perovskite materials has given rise to a large diversity of compounds with signatures related to that of the perovskite. Their

large number makes impossible to describe all of them here. Therefore, in the following lines, we will just give a simplified general insight on the most significant perovskites and perovskite-related structures, organised as stoichiometric, non-stoichiometric and layered perovskites (see summary in Figure 3).

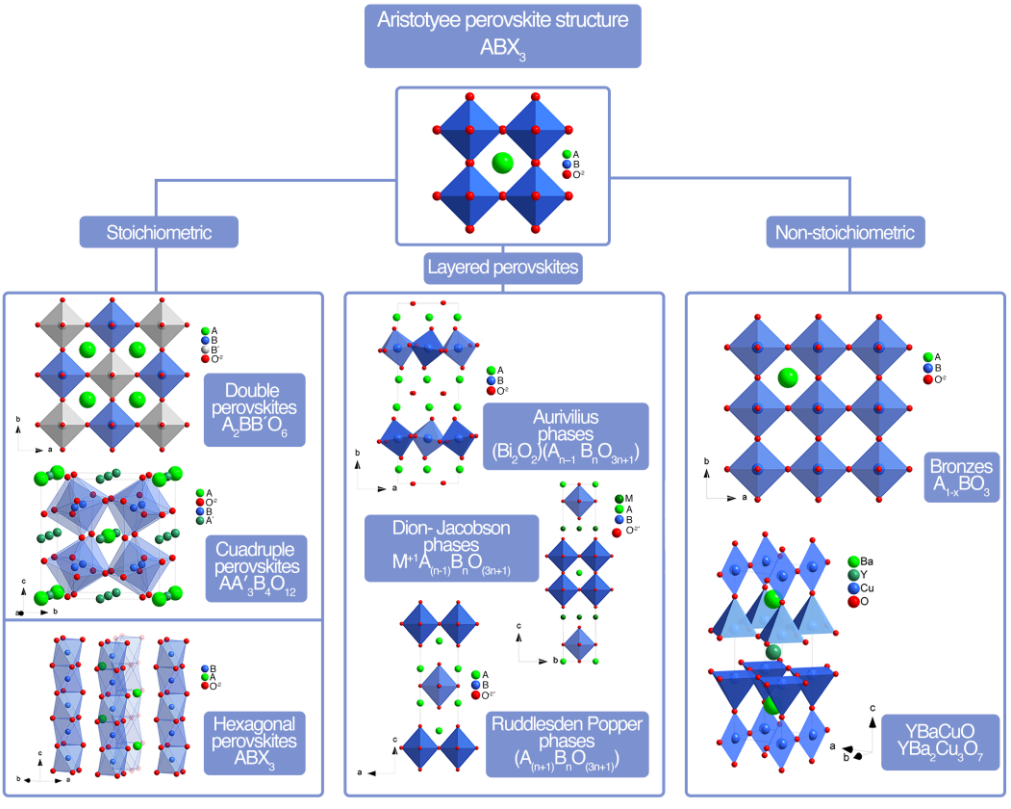

Figure 3: Summary of Perovskite-related structures

II.4 Stoichiometric perovskites and related structures

The main characteristic of this heterogeneous and wide group is the keeping of the ABX_3 stoichiometry.

Out of all of them, in this short presentation we will specifically refer to the case of substituted (also known as doped-) perovskites, all of them based on the cubic close packing of "AX_3" layers, some of them with superstructures derived from the parent compound.

We will also refer to perovskite-related structures based instead on a hexagonal sequence of the "AX_3" layers.

II.5 Substituted perovskites

As already mentioned above, the perovskite is a very flexible structure that allows many substitutions, even partially in the A, B and X sites, with possibility of order/disorder, as we show with the following examples (see also Figure 3):

- **Partial substitutions in the A-site** (with iso or aliovalent substitutions) giving rise to compounds of general formula $A_{1-x}A'_xBX_3$, such as $La_{1-x}Sr_xCoO_3$ (29)
- **Partial substitutions in the B-site** (with iso or aliovalent substitutions) giving rise to compounds of general formula $AB_{1-x}B'_xX_3$, such as $LaCo_{1-x}Mn_xO_3$ (30)
- **Partial substitutions in the X-site** (with iso or aliovalent substitutions) giving rise to compounds of general formula $ABO_{3-x}X_x$, such as $BaTiO_{3-x}H_x$ (31)

It should be noted that, when doping with cations/anions of different charge, the compound electroneutrality should be always maintained. This can be achieved by a simultaneous change in the valence of the other ions present in the lattice (very often transition metal cations sitting in the B-site that allow mixed valence, as in the case of the $La_{1-x}Sr_xCoO_3$ compounds, where the formal average valence of the Co-ions changes from 3+ to 3+x+); or by creating vacancies in the X-sites, see examples below in the non-stoichiometric perovskite-related structures section.

Such substitutions allow very significant changes and modulate the physical properties of the resulting materials. For example, $LaMnO_3$ is an A-type antiferromagnet and electrical insulator, with the Mn^{3+} cations exhibiting an orbital ordering related with a cooperative Jahn-Teller distortion. The substitution of some of the La^{3+} cations in the A-site by divalent cations (such as Ca^{2+}) giving $La_{1-x}Ca_xMnO_3$, induces the partial oxidation of manganese and then the coexistence of trivalent Mn^{3+} and tetravalent Mn^{4+} cations.(19) This doping provokes various complex electron correlation phenomena, such as double exchange, charge/orbital ordering and phase segregation, which are finally responsible for the ferromagnetic, metallic and colossal magnetoresistance properties exhibited by some members of the $La_{1-x}Ca_xMnO_3$ series. (32)

That is why the partial substitution of A- and/or B-cations has been widely used as a simple but very effective strategy for tailoring the properties of oxidic perovskite compounds.

It should also be mentioned that, when different ionic species are occupying the same site, and their charges and/or their ionic sizes are different enough, lattice energy can often be reduced by ordering these ions over the available crystallographic sites.

A particularly interesting case (represented in Figure 3) is when exactly half of the B-site cations are substituted with another B´ cation, giving rise to the so-called B-site ordered double-perovskites $A_2BB´X_6$. (33) Both cations can exhibit different ordered patterns, such as rock-salt (the B-site cations alternate in all three dimensions), or even layered or columnar order. (34)

Another relevant example also shown in Figure 3 is that of quadruple perovskites $AA'_3B_4X_{12}$, which surprisingly have twelve-fold coordinated A-sites and square-planar coordinated A′-sites. (35)

In addition to cation-substituted perovskites, anion-substituted perovskites with multiple anions at the X-site, such as oxyhalides, oxynitrides and oxyhydrides are also currently arising great interest and are being studied with the expectative of superior functionality to the single-oxide ion perovskites. (36)

II.6 Hexagonal perovskite–related structures

One of the largest family of stoichiometric perovskite-related structures are those known as hexagonal perovskites, where the *TF* is higher than 1, and the size of the A-cation is too large to be located at the cubooctahedral cavity of the BX_3 framework.

In the ideal hexagonal perovskite (also called 2H-hexagonal polytype) (see Figure 3), the crystal structure is based on a hexagonal close packing of "AX_3" layers, instead of the cubic sequence of the conventional perovskite structure. The resulting hexagonal polytype consists of infinite columns of face-sharing [BX_6] octahedra interleaved with chains of A cations, both running parallel to the c-axis.

Another more complex hexagonal phases are perovskites with mixed hexagonal and cubic packing, with both face-sharing and corner-sharing octahedra, giving to a large number of polytypes, such as 4H, 6H, 15R and so on. (8)

In addition, hexagonal perovskites can also exhibit partial substitutions in the A, B and X sites, with possibility of order/disorder and even non-stoichiometry.

II.7 Non-stoichiometric perovskite-related structures

The perovskite structure is also very flexible in the sense that it tolerates structural defects, such as A, B or X deficiency. Specially, the perovskite structure exhibits a large tolerance to A-site or X-site deficiencies and even with possibility of order/disorder arrangement of vacancies.

It is worth to note that the X-site deficiencies can be provoked by partial substitutions at the A and/or B sites.

A relevant example of this latter case is the very famous high temperature superconductor "YBaCuO" with chemical formula $YBa_2Cu_3O_{7-\delta}$. Its crystalline structure, shown in Figure 3, is based on an oxygen deficient triple perovskite $3x(ABO_{3-\delta})$, that is $A_3B_3O_{9-\delta}$, with the Y^{+3} and Ba^{+2} cations ordered over the A site and with only 7 oxygen anions per formula unit, instead of the 9 corresponding to the stoichiometric ideal composition. Therefore, the copper atoms are no longer octahedrally coordinated by oxygen ions, but instead part of them have 5 oxygen neighbors in square-pyramidal arrangement, while others have 4 oxygen neighbors in square-planar coordination.(37)(38), see Figure 3 And it is precisely this special oxygen content the one needed for rendering the material superconducting below the highest T_c critical temperature of 92 K. (39)

Relevant examples for A-site-deficient perovskites (which is a common deficiency among tungstates, titanates, niobates and tantalates) are the tungsten bronzes, with general formula A_xWO_3 (40), whose remarkable electrical and optical properties are also related to the structure and special stoichiometry. (41)

II.8 Layered perovskites

Finally, many phases related to the perovskite structure are modular, being built by infinite 2D slabs of a perovskite structure interleaved with other structures, such as rock-salt layers or alkali metal layers.

Among the most common layered perovskites are the following (Figure 3):

- Ruddlesden-Popper phases of general formula $(A_{(n+1)}B_nO_{(3n+1)}$ where n=1, 2, 3, …..∞ indicates the width of the perovskite slabs between the rock-salt layers. (42)(43) The simplest family member has n=1, and is comprised by one perovskite layer interleaved with AO rock salt layers and turns to be a bidimensional structure. Other family members exhibit broader perovskite

slabs along the c-axis, and are therefore compounds with higher dimensionality. Finally The n= ∞ member corresponds to the three dimensional (3D) ABO_3 perovskite.

- Aurivillius phases: their general formula is $(Bi_2O_2)(A_{n-1}B_nO_{3n+1})$ and the intruding layer is composed by $(Bi_2O_2)^{2+}$ blocks. (44)(45)
- Dion-Jacobson phases: their general formula is $M^{+1}A_{(n-1)}B_nO_{(3n+1)}$ and the intruding layer is formed by alkali metal cations M^+. (46)(47)

III. Hybrid perovskites

Exploring further the possibilities of this versatile structure, scientists have created the subclass of perovskite materials known as hybrid organic–inorganic perovskites (HOIPs), which are comprised of organic and inorganic building blocks, also known as “molecular” perovskites, where the A- and/or X-site inorganic moieties of the conventional ABX_3 perovskites have been replaced by molecular ions.(12) The introduction of these molecular ions (even organic components) in the structure of these HOIPs give rise to additional functionalities and structural flexibility that cannot be achieved in purely inorganic perovskites.

Most interestingly, the multiple available combinations offer substantial opportunities for tuning and modulating the physical properties of these compounds by facile chemical modification, (48) opening up enormous possibilities for finding exciting new (multi)functional (49)(50) and (multi)stimuli responsive (51)(52) materials.

The introduction of organic components into the A and/or X-site- the position B is usually occupied by metal cations- gives a large variety of HOIP derivatives (Figure 4). Up to date, several X anions have been used to create hybrid perovskite compounds, such as: (i) monoatomic halogen ions (Cl^-, Br^-, I^-); (ii) diatomic ions, i.e. cyanides (CN^-),(53); (iii) polyatomic ions, i.e. nitrides (N_3^-)(54)(55), formates ($HCOO^-$) (56)(57)(58), thiocyanates (SCN^-) (59), dicyanamides ($N(CN)_2^-$) (60)(52), M-cyanides ($[M(CN)_2]^-$(61), tetrafluoroborates (BF_4^-), phosphates (PO_4^-), phosphinates ($H_2PO_2^-$). (62)(63). Several molecular cations have been located in the A-site (the framework cavities), typically alkylammonium cations or organophosphonium cations (see Figure 4).

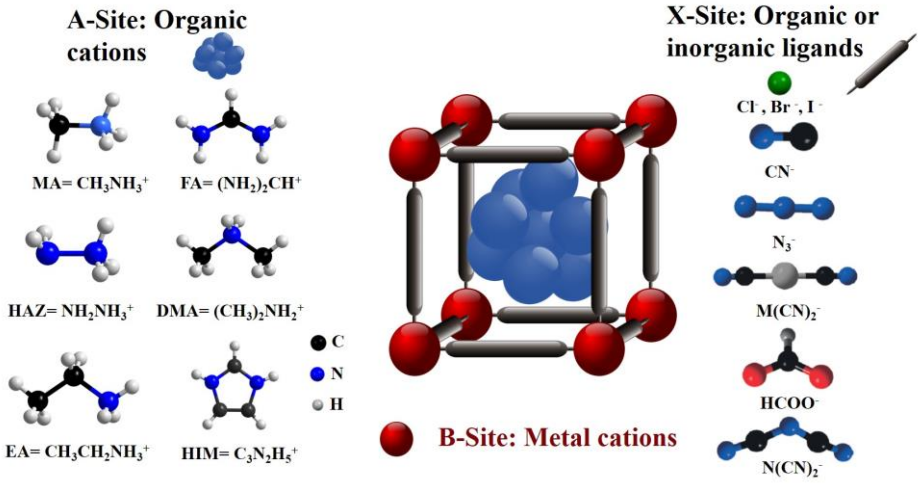

Figure 4: Typical components of organic-inorganic hybrid perovskites. A-sites are normally occupied by midsize organic alkylammonium cations, B-site by metal cations, and X-sites by halogens or organic bidentade-bridging ligands.

III.1 Tolerance factor in hybrid perovskites

Due to the introduction of polyatomic components into the A and/or X-sites, the challenge in determining tolerance factors for organic-inorganic compounds lies in estimating the ionic radii of molecular ions. In the case of hybrid perovskites, we are dealing with polyatomic ions, which are non-spherical, and so an obvious difficulty is encountered in defining the A- and X-site ionic radius for use in tolerance factor equation.

Recently, Kieslich et. al. (64) have extended the tolerance factor concept to the hybrid perovskites to estimate a consistent set of effective radii for different polyatomic ions. In particular, their approach has been assuming rotational freedom around the centre of mass. A rigid sphere model is applicable to molecular A-site cations and leads to a consistent set of effective ionic radii (r_{Aeff}). Equation 3 was used to suggest effective ionic radii for the most common nitrogen based cations (Table 1)

$$r_{Aeff} = r_{mass} + r_{ion} \qquad \text{Eq. 3}$$

with r_{mass} being the distance between the centre of mass of the molecule and the atom with the largest distance to the centre of mass, excluding hydrogen atoms; r_{ion} is the corresponding ionic radius of this atom. This approach gives a set of effective radii that

can be used to estimate tolerance factors. Recently, Becker et al. (65) have proposed a novel approach to assigning more precise ionic radii of molecular cations using computational methods. In this context, to quantify the anisotropic shape of the molecular cation, Goodwin et al. (66) have introduced the asphericity parameter, which allows to estimate if the A-site cation exhibits anisotropic, prolate or oblate shape. For polyatomic anions at the X-site, such as formates ($HCOO^-$), cyanides (CN^-) and nitrides (N_3^-), the situation is still more complicated by the high anisotropic shape of the anions. Therefore, all molecular anions have been treated as rigid cylinders (the yellow cylinders in Figure 5), with effective radius r_{xeff} and an effective height h_{xeff}.(64)

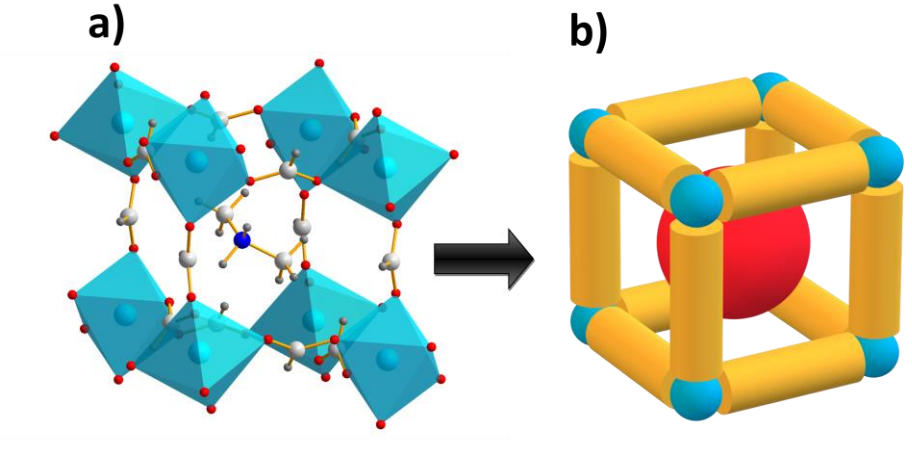

Figure 5: (a) Crystal structure of a formate perovskite with dimethylammonium cations in the cavities of the framework and (b) the corresponding modelled crystal structure to estimate the tolerance factor.

The radius and the height of the cylinder are then evaluated according Equation 3. Therefore, the Equation 1 described above for inorganic perovskites in the previous section, is modified to give Equation 4:

$$TF = \frac{(r_{A_{eff}} + r_{X_{eff}})}{\sqrt{2}\left(r_b + \frac{h_{X_{eff}}}{2}\right)} \qquad \text{Eq. 4}$$

The range of tolerance factor in which the formation of the crystal structure is favorable for hybrid perovskites was estimated experimentally. In this context, Kieslich et. al. (64) have suggested that the range of stability for hybrid halide cubic perovskites is roughly $0.8 \leq t \leq 1$; they tend to form an orthorhombic structure when $t < 0.8$ and a hexagonal structure when $t > 1$. These results are very similar to that found for inorganic perovskites, suggesting a similar significant role of the packing density on the formation of HIOPs and on the inorganic perovskites. In any case, the factors that govern the formation of molecular perovskites are still being explored.

III.2 Distortions of hybrid perovskite structures

As in inorganic perovskites, the mismatch in the size or shape of the A, B and X components yields to structural distortions in the perovskite arrangement. Therefore, the HIOPs can also exhibit B-cation displacement, $[BX_6]$ tilt/rotation and $[BX_6]$ distortions, as previously reported for inorganic perovskites.

Furthermore, the presence of polyatomic components in the HIOPs can give rise to new structural distortions (more or less gradual) and more complicated mechanisms (sometimes associated with specific structural transitions), which are not observed in inorganic perovskites. Hence, the HIOPs have hidden tricks that allow them to make other distortions, unimaginable in their purely inorganic perovskite analogues.

The simplest case is when the A-site is occupied by an organic cation and X is a monoatomic ligand, such as $MAPbX_3$ perovskites where MA is the methylammonium cation and X is one halide (Cl^-, Br^- or I^-). Those hybrid perovskites display two extra mechanisms of structural distortions:

i) Order-disorder of the A cations (Figure 6). The dynamic movement of the organic A cations is defined as *disorder* and thermally activated. Typically, the organic cation is frozen at low temperature without dynamic movement (ordered). On heating, there is a transition of the A cations from the ordered to a disordered state, even with additional transitions between different disordered states. (67)

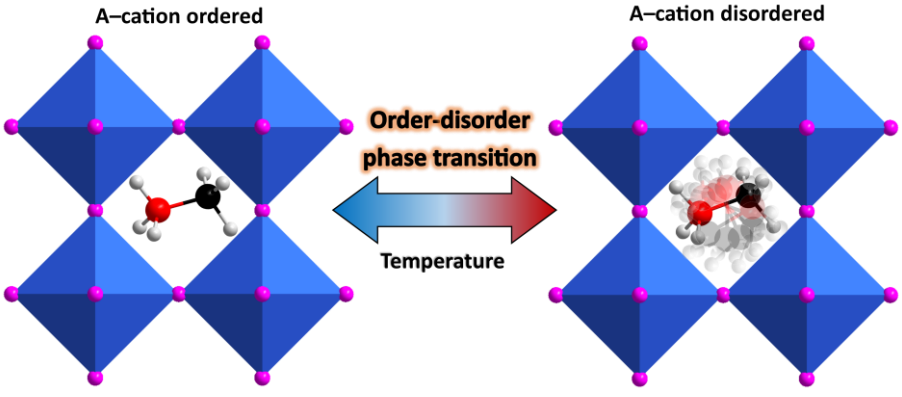

Figure 6: Sketch of the order-disorder transition of the A cation in the Simplest case of hybrid organic inorganic perovskites.

ii) Hydrogen-bonding between the A cations and the framework (Figure 7). This H-bonding provokes a structural distortion in the framework, such as tilting and/or distortions at the [BX_6] octahedra. (67) As the H-bonds become stronger on cooling (and weaker on heating) this mechanism and its consequences are especially relevant at low temperatures.

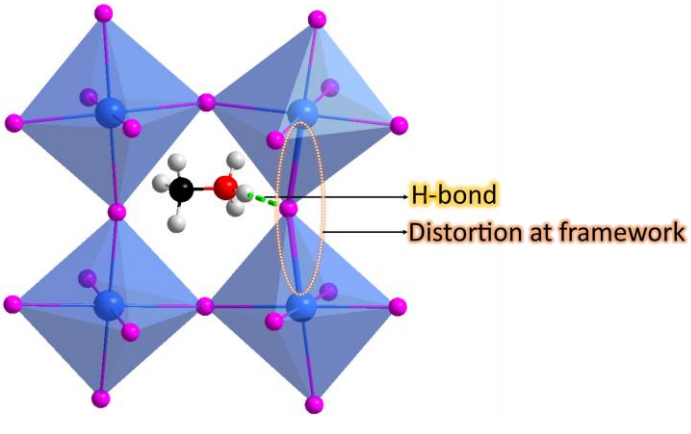

Figure 7: Hydrogen-bonding between the A cation and the framework in the simplest case of hybrid organic inorganic perovskites.

As the X-site evolves from a single atom to a molecular linker, additional factors coming from the increased chemical complexity gain importance and the situation becomes more complicated. Inevitably, the much larger X- anion offers additional degrees of freedom for distortion of the octahedra in HOIPs. Even more, the addition of a molecular linker can also give rise to new structural distortions, such as an order/disorder processes of the anionic linker (Figure 8), similar to those mentioned for the A-site cations.

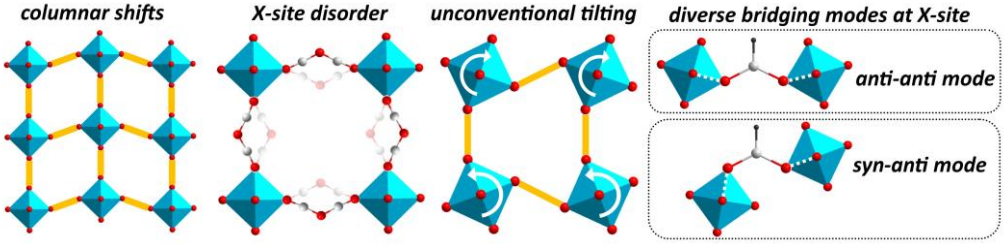

Figure 8: Some of the unique distortion mechanisms reported for hybrid perovskites with X-molecular linkers.

Another interesting feature in hybrid perovskites with polyatomic X-ligands, as compared to the analogue case with monoatomic X-ligands is that they can tolerate larger A,B,X size mismatch, and thus display lower tolerance factor while maintaining the perovskite architecture. As an example, we can mention the case of the Cd-formate perovskite $[NH_4][Cd(HCOO)_3]$, which has a tolerance factor value of t=0.62. (68) We believe that this unusually low tolerance factor has been stabilized in this compound with perovskite-like structure thanks to a change in the coordination mode of the $HCOO^-$ ligand, which can display both *syn-anti* or *anti-anti* configuration (Figures 8 and 9).(69) In this case, the change from the usual *anti-anti* mode to *syn-anti* configuration allows a change at the volume of the cubooctahedral cavity (Figure 9) for a better size matching of the A and B cations. (68) This diverse bridging mode is observed in other polyatomic ligands, such as N_3^-, OCN^-, SCN^-, $N(CN)_2^-$, etc.

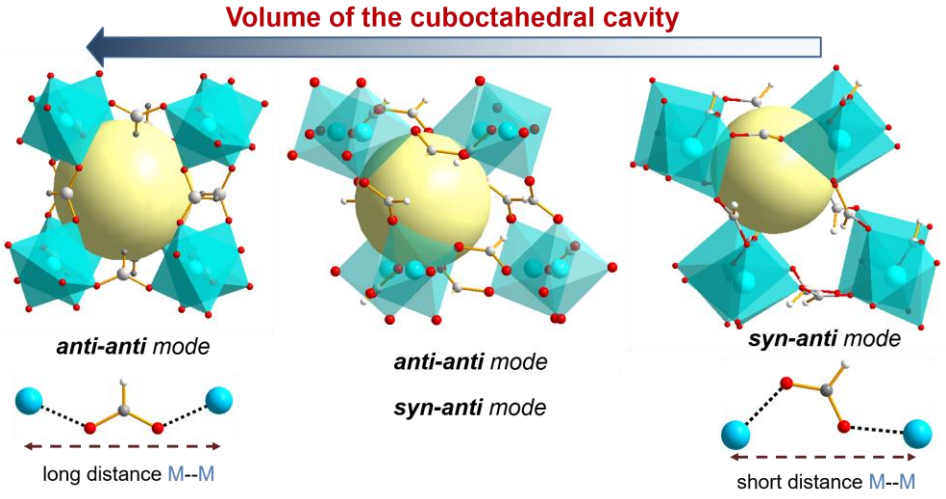

Figure 9: Variation of the volume of the cuboctahedral cavity of perovskites depending on the mode of coordination of the X-site ligands.

In addition to the possibility of a change of the linker bridging mode and the order-disorder transitions of the anionic linkers, the hybrid perovskites with polyatomic ligands display more unique distortion mechanisms, such as "forbidden or unconventional" tilt systems (55), in which the coordination octahedra rotate in the same direction (Figure 8) (which is not allowed in inorganic and monoatomic X-ligand perovskites, where the neighbouring octahedra rotate in alternating directions) (Figure 2) or other in which a columnar shift takes place (70) (Figure 8).

Figure 10 summarizes all the distortion mechanisms reported for hybrid perovskites, compared to the case of inorganic perovskites.

Another important remark is that as the perovskite components evolve from single atoms to polyatomic ions/molecules, the resulting compounds become more complicated from a structural point of view, and different configurations become available with low energy differences between them. Very interestingly, such structural richness provoke that the hybrid perovskites can easily display structural phase transitions by the application of external stimuli such as temperature, pressure, light, etc.

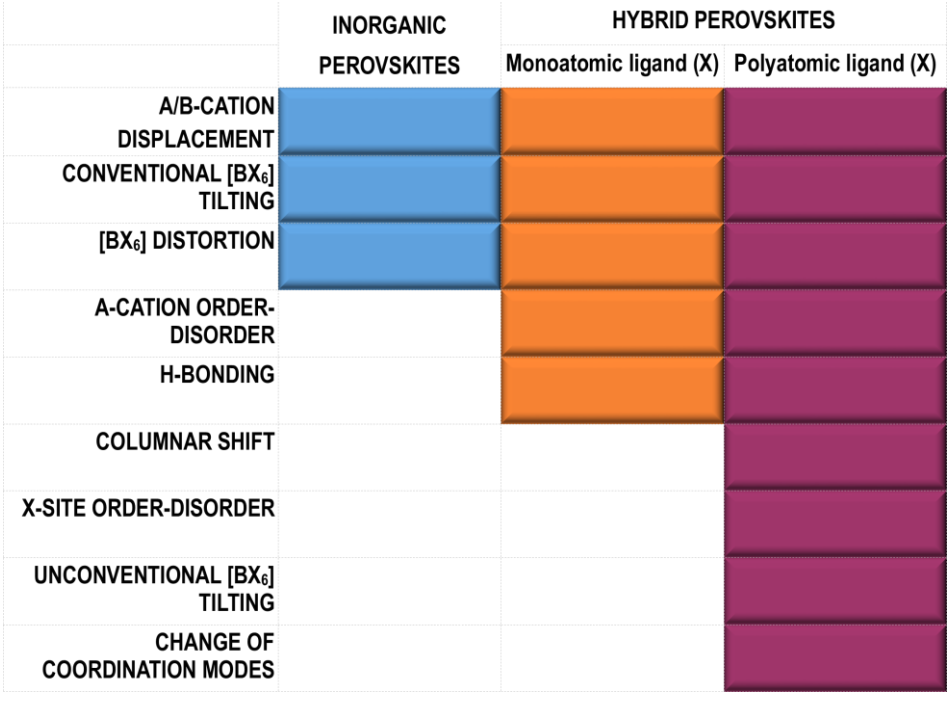

Figure 10: Classification of the distortion mechanisms reported for inorganic and hybrid perovskites.

In this context, the structural phase transitions can play an important role on the physical properties of these materials. Moreover, the different structural distortions are not mutually exclusive, and they can often occur in combination with each other. This coupling of the structural distortions has a crucial role in coupling different functional properties and allowing to obtain multiferroic materials.

For example, when the A-site organic cations are polar (for example, methylammonium (MA) or dimethylammonium (DMA)), and their specific alignments often induced by hydrogen bonding cause bulk electric ordering, the hybrids can exhibit ferroelectricity.(71) In fact, ferroelectricity is more frequently observed in hybrid perovskites than in inorganic perovskites.(72) Moreover, the diverse structural distortions in the hybrid perovskites induce more easily the loss of the inversion centre.(73) In addition, if the framework of the hybrid perovskite exhibits long range magnetic ordering, and the polar A-cation is linked to it by a H-bond, both the magnetic and polar arrangements can couple to give a multiferroic behaviour. (50) (71)

Other interesting properties related to phase transitions are caloric effects. In fact, the hybrid perovskites exhibit the basic ingredients to display large caloric effects, namely large and reversible entropy changes commonly related to order–disorder phase transitions, as well as remarkable external multi-stimuli responses (towards magnetic and/or electric field, pressure, temperature, and so on). This effect can be especially strong in the case of applying pressure due to the rather high flexible structures of the hybrid perovskites. (51)(74)

Beyond the interesting properties associated with phase transitions, HOIPs offer other new properties. For example, hybrid halide perovskites exhibit unprecedented optoelectronic properties, showing impressive performance in solar cells,(75) light emitting diodes,(76) lasers,(77), ultraviolet-to-infrared photodetectors (78) and X-ray (79) and γ-ray detectors.(80) Their success is related to their incredible properties, such as, high optical absorption coefficient over the whole visible range, long carrier diffusion lengths (suppressed recombination and defect tolerance), low exciton binding energy, large dielectric constant and high carrier mobility.(81) Even if the origin of the exceptional photovoltaic (PV) characteristics of the hybrid photovoltaic perovskites is still unknown, hybrid perovskites only contains generally shallow traps defects, benign grain boundaries, low exciton binding energy, large photon recycling, existence of ferroelectric domains and ion migration favouring large diffusion coefficients of carriers, extraordinary absorption coefficient or a combination of all the aforementioned, in where it is clear that the crystal structure has a fundamental role. Even the organic cation, not participating directly in the valence and conduction energy bands of the inorganic framework, it has a templating indirect effect which is able to modulate the bandgap of the hybrid material.

III.3 Hybrid perovskite-related structures

Similarly to what happens in the case of inorganic perovskites, HIOPs exhibit phases related to the perovskite structure, such as hexagonal perovskites, B-site ordered double-perovskites and layered perovskites. As we have previously indicated, when the tolerance factor is larger than 1, the hexagonal perovskite structure becomes more favourable than the cubic one. In this context, different hybrid hexagonal perovskite

polytypes have been reported in the literature (82), such as the 2H, 4H, 6H and 9R[1], although the 2H- and 4H-polytype seems to be the most common.(83)(84) A non-stoichiometric crystal structure related to the 2H polytype has also been described. Another interesting crystal structure has a general formula $A_3B_2X_9$, where the B-site is occupied by a trivalent cation together with ordered vacancies in this site, and where the 2H-types linear chains of face-sharing $[BX_6]$ octahedra becomes into insulated B_2X_9 dimers at the $A_3B_2X_9$ compounds.(85)

Taking into account electroneutrality and typically HIOPs having A and X monovalent ion, then the B cations must be divalent. This valence can be achieved not only by using M^{2+} cations but also by employing equimolar numbers of monovalent and trivalent cations. Typically, this type of perovskite with two cations of different charge and ionic radii are ordered and give rise to the so-called B-site ordered double-perovskite (86). In this case, the force that causes the ordering of the cations is the great difference of charge and size of the two B cations.

The HIOPs can exhibit a novel mechanism to promote the cation ordering, which is related to the chemical properties of the X anion. For example, the thiocyanate ligand SCN^- is an ambidentate ligand,[2] which can act as nucleophile at either sulphur or nitrogen. Nevertheless, strong acid metals tend to favour the link by its N atom, while soft acid metals tend to favoured the link by the S atom. By this strategy, Xie et al. (59) have obtained a double perovskite-type $[NH_4]_2[NiCd(SCN)_6]$ with two different divalent cations.

Finally, hybrid layered perovskites are the most extended family of hybrid perovskite-related structure. (87) In this latter family there are not restrictions for the size of the A-cation, although there is a restriction for the width, which must fit into the volume defined by the terminal halides from four adjacent corner-sharing octahedra. In these compounds, the corner- sharing $[BX_6]$ octahedra are maintained only within perovskite slabs, which appear intergrowth and separated by layers of typically large organic cations. In fact, different families of hybrid layered perovskites are known with perovskite slabs -of different thickness, see below- oriented along different crystallographic directions, as shown in Figure 11 (88):

---

[1] This is the Ramsdell notation, which gives the number of layers (2, 4 ,6 or 9) in the crystallographic repeat, together with the symmetry of the unit cell, specified by H for hexagonal and R for rhombohedral.

[2] Ligands, such as SCN^-, that can bond to a central atom through either of two or more donor atoms are termed ambidentate.

- The family of ⟨100⟩-oriented layered perovskites with general formula of $(RNH_3)_2A_{n-1}B_nX_{3n+1}$.
- The family of ⟨110⟩-oriented layered perovskites with general formula of $A'_2A_mB_mX_{3m+2}$.
- The family of ⟨111⟩-oriented layered perovskites with general formula of $A'_2A_{q-1}B_qX_{3q+3}$,

In all this cases the number of perovskite layers (m, n, q) within the perovskite slabs can be modified from 1 to ∞ (perovskite structure) giving rise to different subfamilies.

This structural flexibility and tunability of the dimensionality also provides a wide diversity for the preparation of interesting crystal structures with varying physical properties at layered perovskites. (89)

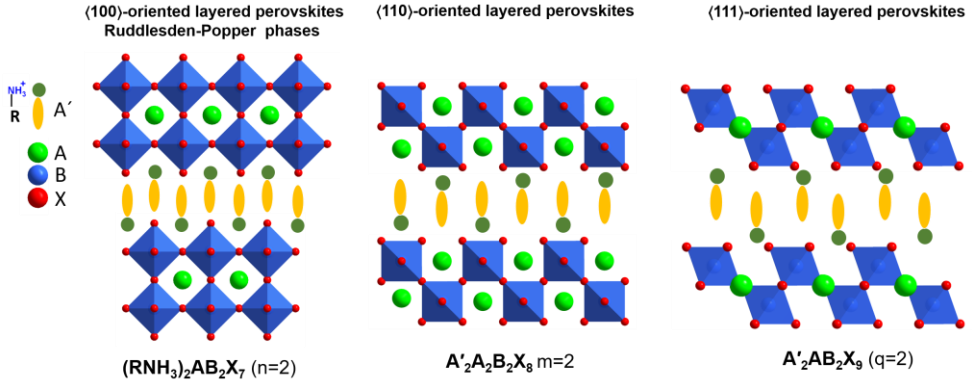

Figure 11: Subfamilies of hybrid layered perovskites separated by a layer of typically large organic cations.

Historically, the hybrid layered perovskites have been dominated by the previously described layered structures, until very recently, where several Dion-Jacobson hybrid layered perovskites have been reported for the first time.(90) The DJ perovskites have a general formula of $AB_{n-1}M_nX_{3n+1}$ with A is a large divalent organic spacers and B is a small monovalent cation.(91) Another very recent discovery is the unprecedented stoichiometry $A_7B_4X_{15}$ showing a 2D layered perovskite structure formed by distorted $[BX_6]$ octahedra sharing corners and phases. (92) Therefore, the recent progress on hybrid layered perovskites has clearly shown that there is plenty of room for the discovery of new materials. (89)

IV. Conclusions

Along the latest decades, pure inorganic perovskites, particularly, oxidic perovskites have been intensively studied due to their interesting functional properties. From these studies, important knowledge has been obtained about chemical and structure-property relationships and this has led the way to design new materials with perovskite structure and related structures with optimized properties.

Recently, hybrid organic-inorganic perovskites are in the spotlight with novel and interesting properties, opening a new route to obtain functional and even multifunctional materials. To enhance rapid advances in the field, the expertise acquired in the study of pure inorganic perovskites, particularly oxidic perovskites, can be a reference of great help. Also, it is necessary to take into account the structural peculiarities that arise with the use of molecular components, and that many of these structural novelties are still unexplored. In any case, the progress already made is very promising and has allowed to understand some of the interesting properties of the hybrid perovskites and even the design of improved hybrid materials. Therefore, the combination of interesting (multi)functional properties and low cost processing, reveals a bright future for hybrid perovskites and their use in the next generation of technological devices and many energy and environmental applications.

Acknowledgements:

This work was financially supported by the Ministerio de Economía y Competitividad (MINECO) and EU-FEDER under the project MAT2017-86453-R and Xunta de Galicia under the project ED431G/09. A. García-Fernández acknowledges Carl Tryggers Stiftelse for a Postdoctoral Fellowship.

Complementary informations on authors:

Alberto García Fernández ORCID: 0000-0003-1671-9979

Emilio Jose Juarez-Perez ORCID: 0000-0001-6040-1920

Socorro Castro-García ORCID: 0000-0003-1501-2410

Manuel Sánchez-Andújar ORCID: 0000-0002-3441-0994

María Antonia Señarís-Rodríguez ORCID: 0000-0002-0117-6855

Cite this paper: A. García-Fernández, E.J. Juárez-Pérez, S. Castro-García, M. Sánchez-Andújar, M.A. Señarís-Rodríguez, OAJ Materials and Devices, vol 5(1) – chap.4 in "*Perovskites and other framework structure crystalline materials*" (Coll. Acad. 2021) DOI:10.23647/ca.md20202205

REFERENCES

1. Galasso FS. Structure, properties, and preparation of perovskite-type compounds. Oxford: Pergamon Press; 1969.
2. Lines ME, Glass AM. Principles and Applications of Ferroelectrics and Related Materials. Oxford University Press; 2001.
3. Goodenough JB. Magnetism and the Chemical Bond. John Wiley & Sons, Ltd; 1963.
4. Rao CNR. Chemistry of High Temperature Superconductors. WORLD SCIENTIFIC; 1991.
5. Liu H, Yang X. A brief review on perovskite multiferroics. Ferroelectrics. 2017, 507, 69–85.
6. Rao CNR, Raveau B. Colossal Magnetoresistance, Charge Ordering and Related Properties of Manganese Oxides. WORLD SCIENTIFIC; 1998.

7. Tejuca LG, Fierro JLG. Properties and applications of perovskite-type oxides. M. Dekker; 1993. 382 p.
8. Tilley RJD. Perovskites: structure-property relationships. Chichester, UK: John Wiley & Sons, Ltd; 2016.
9. Goodenough JB, Longo M. Magnetic and Other Properties of Oxides and Related Compounds. Landolt-Börnstein - Group III Condensed Matter·Volume 4A. Hellwege K-H, Hellwege AM, editors. Springer-Verlag Berlin Heidelberg; 1970.
10. Reller A, Williams T. Perovskites. Chemical chameleons. Chem Britain. 1989, 25, 1227–30.
11. West AR. Perovskite: A Solid-State Chemistry Chameleon, Illustrating the Elements, Their Properties and Location in the Periodic Table. In Springer, Berlin, Heidelberg; 2019, p. 1–32.
12. Li W, Wang Z, Deschler F, Gao S, Friend RH, Cheetham AK. Chemically diverse and multifunctional hybrid organic–inorganic perovskites. Nat Rev Mater. 2017; 2, 16099.
13. Wang ZL, Kang ZC. Functional and Smart Materials. Boston, MA: Springer US; 1998
14. Dang Y, Ju D, Wang L, Tao X. Recent progress in the synthesis of hybrid halide perovskite single crystals. CrystEngComm. 2016, 18, 4476–84.
15. Shamsi J, Urban AS, Imran M, De Trizio L, Manna L. Metal Halide Perovskite Nanocrystals: Synthesis, Post-Synthesis Modifications, and Their Optical Properties. Chem Rev. 2019, 119, 3296–348.
16. Mitchell RH. Perovskites : modern and ancient. Almaz Press; 2002, 318 p.
17. Navrotsky A, Weidner DJ. Perovskite : a structure of great interest to geophysics and materials science. American Geophysical Union; 1989. 146 p.
18. Von Hippel A. Ferroelectricity, Domain Structure, and Phase Transitions of Barium Titanate. Rev Mod Phys. 1950, 22, 221–37.
19. Jonker GH, Van Santen JH. Ferromagnetic compounds of manganese with perovskite structure. Physica. 1950, 16, 337–49.
20. Goodenough JB. Theory of the Role of Covalence in the Perovskite-Type Manganites [La,M(II)] MnO_3. Phys Rev. 1955, 100, 564–73.

21. Hazen RM, Finger LW, Angel RJ, Prewitt CT, Ross NL, Mao HK, et al. Crystallographic description of phases in the Y-Ba-Cu-O superconductor. Phys Rev B. 1987, 35, 7238–41.
22. Levy PM, Tiefel TH, McCormack M, Fastnacht RA, Ramesh R, Chen LH. Giant magnetoresistance in magnetic layered and granular materials. Science. 1992, 256, 972–3.
23. Peña MA, Fierro JLG. Chemical Structures and Performance of Perovskite Oxides. Chem Rev. 2001, 101, 1984–2018.
24. Megaw HD. Crystal structure of double oxides of the perovskite type. Proc Phys Soc. 1946, 58, 133–52.
25. Goldschmidt VM. Die Gesetze der Krystallochemie. Naturwissenschaften. 1926, 14, 477–85.
26. Bartel CJ, Sutton C, Goldsmith BR, Ouyang R, Musgrave CB, Ghiringhelli LM, et al. New tolerance factor to predict the stability of perovskite oxides and halides. Sci Adv. 2019, 5, 1–10.
27. Glazer AM. The classification of tilted octahedra in perovskites. Acta Crystallogr Sect B Struct Crystallogr Cryst Chem. 1972, 28, 3384–92.
28. Goodenough JB. Electronic and ionic transport properties and other physical aspects of perovskites. Reports Prog Phys. 2004, 67, 1915–93.
29. Señarís-Rodríguez MA, Goodenough JB. Magnetic and Transport Properties of the System $La_{1-x}Sr_xCo_{O3-\delta}$. J Solid State Chem. 1995, 118, 323–36.
30. Goodenough J, Wold A, Arnott R, Menyuk N. Relationship Between Crystal Symmetry and Magnetic Properties of Ionic Compounds Containing Mn^{3+}. Phys Rev. 1961, 124, 373–84.
31. Kobayashi Y, Hernandez OJ, Sakaguchi T, Yajima T, Roisnel T, Tsujimoto Y, et al. An oxyhydride of $BaTiO_3$ exhibiting hydride exchange and electronic conductivity. Nat Mater. 2012, 11, 507–11.
32. Tokura Y (Yoshinori). Colossal magnetoresistive oxides. Gordon and Breach Science Publishers; 2000, 358 p.
33. Vasala S, Karppinen M. $A_2B'B''O_6$ perovskites: A review. Vol. 43, Progress in Solid State Chemistry. Pergamon; 2015. p. 1–36.
34. Anderson MT, Greenwood KB, Taylor GA, Poeppelmeier KR. B-cation arrangements in double perovskites. Prog Solid State Chem. 1993, 22,

197–233.

35. Belik AA. Rise of A-site columnar-ordered $A_2A'A''B_4O_{12}$ quadruple perovskites with intrinsic triple order. Dalt Trans. 2018, 47, 3209–17.
36. Kageyama H, Hayashi K, Maeda K, Attfield JP, Hiroi Z, Rondinelli JM, et al. Expanding frontiers in materials chemistry and physics with multiple anions. Nat Commun. 2018, 9, 772.
37. Park C, Snyder RL. Structures of High-Temperature Cuprate Superconductors. J Am Ceram Soc. 1995, 78, 3171–94.
38. Santoro A, Beech F, Marezio M, Cava RJ. Crystal chemistry of superconductors: A guide to the tailoring of new compounds. Phys C Supercond. 1988, 156, 693–700.
39. Khare N. Handbook of high-temperature superconductor electronics. Marcel Dekker; 2003.
40. Dickens PG, Whittingham MS. The tungsten bronzes and related compounds. Q Rev Chem Soc. 1968, 22, 30–44.
41. Rao CNR, Gopalakrishnan J. New Directions in Solid State Chemistry. second. Cambridge: Cambridge University Press; 1997.
42. Ruddlesden SN, Popper P. The compound $Sr_3Ti_2O_7$ and its structure. Acta Crystallogr. 1958, 11, 54–5.
43. Beznosikov B V., Aleksandrov KS. Perovskite-like crystals of the Ruddlesden-Popper series. Crystallogr Reports. 2000, 45, 792–8.
44. AURIVILLIUS, B. Mixed Bismuth Oxides with Layer Lattices I. The Structure Type of $CaNb_2Bi_2O_9$. Ark Kemi. 1949, 1, 463–80.
45. Kendall KR, Navas C, Thomas JK, zur Loye H-C. Recent Developments in Oxide Ion Conductors: Aurivillius Phases. Chem Mater. 1996, 8, 642–9.
46. Dion M, Ganne M, Tournoux M. Nouvelles familles de phases MIMII2Nb3O10 a feuillets “perovskites.” Mater Res Bull. 1981, 16, 1429–35.
47. Jacobson AJ, Johnson JW, Lewandowski JT. Interlayer chemistry between thick transition-metal oxide layers: synthesis and intercalation reactions of $K[Ca_2Na_{n-3}Nb_nO_{3n+1}]$. Inorg Chem. 1985, 24, 3727–9.
48. Cheetham AK, Rao CNR. There’s Room in the Middle. Science. 2007, 318, 58–9.

49. Di Sante D, Stroppa A, Jain P, Picozzi S. Tuning the Ferroelectric Polarization in a Multiferroic Metal–Organic Framework. J Am Chem Soc. 2013, 135, 18126–30.

50. Gómez-Aguirre LC, Pato-Doldán B, Mira J, Castro-García S, Señarís-Rodríguez MA, Sánchez-Andújar M, et al. Magnetic Ordering-Induced Multiferroic Behavior in $[CH_3NH_3][Co(HCOO)_3]$ Metal–Organic Framework. J Am Chem Soc. 2016, 138, 1122–5.

51. Bermúdez-García JM, Sánchez-Andújar M, Señarís-Rodríguez MA. A New Playground for Organic–Inorganic Hybrids: Barocaloric Materials for Pressure-Induced Solid-State Cooling. J Phys Chem Lett. 2017, 8, 4419–23

52. Bermúdez-García JM, Sánchez-Andújar M, Yáñez-Vilar S, Castro-García S, Artiaga R, López-Beceiro J, et al. Multiple phase and dielectric transitions on a novel multi-sensitive $[TPrA][M(dca)_3]$ (M: Fe^{2+}, Co^{2+} and Ni^{2+}) hybrid inorganic–organic perovskite family. J Mater Chem C. 2016, 4, 4889–98.

53. Zhang W, Cai Y, Xiong R-G, Yoshikawa H, Awaga K. Exceptional Dielectric Phase Transitions in a Perovskite-Type Cage Compound. Angew Chemie Int Ed. 2010, 49, 6608–10.

54. Mautner FA, Cortés R, Lezama L, Rojo T. $[N(CH_3)_4][Mn(N_3)_3]$: A Compound with a Distorted Perovskite Structure through Azido Ligands. Angew Chemie Int Ed English. 1996 35, 78–80.

55. Gómez-Aguirre LC, Pato-Doldán B, Stroppa A, Yang L-M, Frauenheim T, Mira J, et al. Coexistence of Three Ferroic Orders in the Multiferroic Compound $[(CH_3)_4N][Mn(N_3)_3]$ with Perovskite-Like Structure. Chem - A Eur J. 2016, 22, 7863–70.

56. Wang X-Y, Gan L, Zhang S-W, Gao S. Perovskite-like Metal Formates with Weak Ferromagnetism and as Precursors to Amorphous Materials. Inorg Chem. 2004, 43, 4615–25.

57. Jain P, Dalal NS, Toby BH, Kroto HW, Cheetham AK. Order−Disorder Antiferroelectric Phase Transition in a Hybrid Inorganic−Organic Framework with the Perovskite Architecture. J Am Chem Soc. 2008, 130, 10450–1.

58. Sánchez-Andújar M, Presedo S, Yáñez-Vilar S, Castro-García S, Shamir J, Señarís-Rodríguez M a. Characterization of the order-disorder

dielectric transition in the hybrid organic-inorganic perovskite-like formate $Mn(HCOO)_3[(CH_3)_2NH_2]$. Inorg Chem. 2010, 49, 1510–6.

59. Xie K-P, Xu W-J, He C-T, Huang B, Du Z-Y, Su Y-J, et al. Order–disorder phase transition in the first thiocyanate-bridged double perovskite-type coordination polymer: $[NH_4]_2[NiCd(SCN)_6]$. CrystEngComm. 2016, 18, 4495–8.
60. Schlueter J a, Manson JL, Geiser U. Structural and magnetic diversity in tetraalkylammonium salts of anionic $M[N(CN)_2]^{3-}$ (M = Mn and Ni) three-dimensional coordination polymers. Inorg Chem. 2005, 44, 3194–202.
61. Hill JA, Thompson AL, Goodwin AL. Dicyanometallates as Model Extended Frameworks. J Am Chem Soc. 2016, 138, 5886–96.
62. Sun Y-L, Han X-B, Zhang W. Structural Phase Transitions and Dielectric Switching in a Series of Organic-Inorganic Hybrid Perovskites ABX_3 ($X=ClO^{4-}$ or BF^{4-}). Chem. A Eur J . 2017, 23, 11126–32.
63. Evans HA, Deng Z, Collings IE, Wu Y, Andrews JL, Pilar K, et al. Polymorphism in $M(H_2PO_2)_3$ (M = V, Al, Ga) compounds with the perovskite-related ReO_3 structure. Chem Commun. 2019, 55, 2964–7.
64. Kieslich G, Sun S, Cheetham T. An Extended Tolerance Factor Approach for Organic-Inorganic Perovskites. Chem Sci. 2015
65. Becker M, Klüner T, Wark M. Formation of hybrid ABX_3 perovskite compounds for solar cell application: First-principles calculations of effective ionic radii and determination of tolerance factors. Dalt Trans. 2017
66. Collings IE, Hill JA, Cairns AB, Cooper RI, Thompson AL, Parker JE, et al. Compositional dependence of anomalous thermal expansion in perovskite-like ABX_3 formates. Dalt Trans. 2016, 45, 4169–78.
67. Weller MT, Weber OJ, Henry PF, Di Pumpo AM, Hansen TC. Complete structure and cation orientation in the perovskite photovoltaic methylammonium lead iodide between 100 and 352 K. Chem Commun. 2015, 51, 4180–3.
68. Gómez-Aguirre LC, Pato-Doldán B, Stroppa A, Yáñez-Vilar S, Bayarjargal L, Winkler B, et al. Room-Temperature Polar Order in $[NH_4][Cd(HCOO)_3]$ A Hybrid Inorganic–Organic Compound with a Unique Perovskite Architecture. Inorg Chem. 2015, 54, 2109–16.

69. Carrell CJ, Carrell HL, Erlebacher J, Glusker JP. Structural aspects of metal ion carboxylate interactions. J Am Chem Soc. 1988, 110, 8651–6.

70. Boström HLB, Hill JA, Goodwin AL. Columnar shifts as symmetry-breaking degrees of freedom in molecular perovskites. Phys Chem Chem Phys. 2016;18, 31881–94.

71. Jain P, Ramachandran V, Clark RJ, Hai DZ, Toby BH, Dalal NS, et al. Multiferroic behavior associated with an order-disorder hydrogen bonding transition in metal-organic frameworks (MOFs) with the perovskite ABX_3 architecture. J Am Chem Soc. 2009,131, 13625–7.

72. Jain P, Stroppa A, Nabok D, Marino A, Rubano A, Paparo D, et al. Switchable electric polarization and ferroelectric domains in a metal-organic-framework. Quantum Mater. 2016, 1, 16012.

73. Boström HLB, Senn MS, Goodwin AL. Recipes for improper ferroelectricity in molecular perovskites. Nat Commun. 2018, 9, 2380.

74. Bermúdez-García JM, Sánchez-Andújar M, Castro-García S, López-Beceiro J, Artiaga R, Señarís-Rodríguez MA. Giant barocaloric effect in the ferroic organic-inorganic hybrid [TPrA][Mn(dca) $_3$] perovskite under easily accessible pressures. Nat Commun. 2017, 8, 15715.

75. Kojima A, Teshima K, Shirai Y, Miyasaka T. Organometal halide perovskites as visible-light sensitizers for photovoltaic cells. J Am Chem Soc. 2009, 131, 6050–1.

76. Tan Z-K, Moghaddam RS, Lai ML, Docampo P, Higler R, Deschler F, et al. Bright light-emitting diodes based on organometal halide perovskite. Nat Nanotechnol. 2014, 9, 687–92.

77. Xing G, Mathews N, Lim SS, Yantara N, Liu X, Sabba D, et al. Low-temperature solution-processed wavelength-tunable perovskites for lasing. Nat Mater. 2014, 13, 476–80.

78. Fang Y, Dong Q, Shao Y, Yuan Y, Huang J. Highly narrowband perovskite single-crystal photodetectors enabled by surface-charge recombination. Nat Photonics. 2015, 9, 679–86.

79. Wei H, Fang Y, Mulligan P, Chuirazzi W, Fang H-H, Wang C, et al. Sensitive X-ray detectors made of methylammonium lead tribromide perovskite single crystals. Nat Photonics. 2016, 10, 333–9.

80. Yakunin S, Dirin DN, Shynkarenko Y, Morad V, Cherniukh I, Nazarenko O, et al. Detection of gamma photons using solution-grown single

crystals of hybrid lead halide perovskites. Nat Photonics. 2016, 10, 585–9.

81. Kumar Jena A, Kulkarni A, Miyasaka T. Halide Perovskite Photovoltaics: Background, Status, and Future Prospects. Chem Rev. 2018.
82. Stoumpos CC, Mao L, Malliakas CD, Kanatzidis MG. Structure–Band Gap Relationships in Hexagonal Polytypes and Low-Dimensional Structures of Hybrid Tin Iodide Perovskites. Inorg Chem. 2017, 56, 56–73.
83. García-Fernández A, Bermúdez-García JM, Castro-García S, Llamas-Saiz AL, Artiaga R, López-Beceiro J, et al. Phase Transition, Dielectric Properties, and Ionic Transport in the $[(CH_3)_2NH_2]PbI_3$ Organic–Inorganic Hybrid with 2H-Hexagonal Perovskite Structure. Inorg Chem. 2017, 56, 4918–27.
84. García-Fernández A, Juarez-Perez EJ, Bermúdez-García JM, Llamas-Saiz AL, Artiaga R, López-Beceiro JJ, et al. Hybrid lead halide $[(CH_3)_2NH_2]PbX_3$ (X = Cl^- and Br^-) hexagonal perovskites with multiple functional properties. J Mater Chem C. 2019
85. Aleksandrov KS, Beznosikov V V. Hierarchies of perovskite-like crystals (Review). Phys Solid State. 1997, 39, 695–715.
86. Wei F, Deng Z, Sun S, Xie F, Kieslich G, Evans DM, et al. The synthesis, structure and electronic properties of a lead-free hybrid inorganic–organic double perovskite $(MA)_2KBiCl_6$ (MA = methylammonium). Mater Horiz. 2016, 6.
87. Mitzi DB. Synthesis, Structure, and Properties of Organic-Inorganic Perovskites and Related Materials. In Wiley-Blackwell; 2007, p. 1–121.
88. Saparov B, Mitzi DB. Organic–Inorganic Perovskites: Structural Versatility for Functional Materials Design. Chem Rev. 2016, 116, 4558–96.
89. Mao L, Stoumpos CC, Kanatzidis MG. Two-Dimensional Hybrid Halide Perovskites: Principles and Promises. J Am Chem Soc. 2019, 141, 1171–90.
90. Mao L, Ke W, Pedesseau L, Wu Y, Katan C, Even J, et al. Hybrid Dion–Jacobson 2D Lead Iodide Perovskites. J Am Chem Soc. 2018, 140, 3775–83.

91. Li Y, Milić J V., Ummadisingu A, Seo J-Y, Im J-H, Kim H-S, et al. Bifunctional Organic Spacers for Formamidinium-Based Hybrid Dion–Jacobson Two-Dimensional Perovskite Solar Cells. Nano Lett. 2019, 19, 150–7.

92. García-Fernández A, Bermúdez-García JM, Castro-García S, Llamas-Saiz AL, Artiaga R, López-Beceiro JJ, et al. $[(CH_3)_2NH_2]_7Pb_4X_{15}$ ($X = Cl^-$ and Br^-), 2D-Perovskite Related Hybrids with Dielectric Transitions and Broadband Photoluminiscent Emission. Inorg Chem. 2018, 57, 3215–22.